INSTITUTE OF PHYSICS PUBLISHING SEMICONDUCTOR SCIENCE AND TECHNOLOGY

Semicond. Sci. Technol. **21** (2006) 1125–1131 doi:10.1088/0268-1242/21/8/025

Influence of annealing on physical properties of evaporated SnS films

M Devika[1], N Koteeswara Reddy[2], K Ramesh[2], K R Gunasekhar[3], E S R Gopal[2] and K T Ramakrishna Reddy[1]

[1] Department of Physics, Sri Venkateswara University, Tirupati 517 502, India
[2] Department of Physics, Indian Institute of Science, Bangalore 560 012, India
[3] Department of Instrumentation, Indian Institute of Science, Bangalore 560 012, India

E-mail: ktrkreddy@hotmail.com

Received 2 May 2006, in final form 14 June 2006
Published 10 July 2006
Online at stacks.iop.org/SST/21/1125

Abstract

The effect of annealing on the composition, crystal structure, surface features and electro-optical properties of tin mono-sulfide (SnS) films, deposited by thermal evaporation at 300 °C, has been studied. Elemental analysis of the films shows sulfur deficiency, which increases at higher annealing temperatures (T_a). The SnS structure in the as-deposited and annealed films remains orthorhombic. With an increase in T_a, the grain size and the surface roughness are reduced. The electrical resistivity also decreases with increasing T_a. The variation of activation energy and optical parameters with T_a has been explained by taking into account the degree of preferred orientation of the grains. The films annealed at 100 °C show some unusual features compared to those annealed at other temperatures.

1. Introduction

During the last two decades, many studies have been made on tin mono-sulfide (SnS) because of various applications in the field of optoelectronics. This compound has an orthorhombic structure, as studied by Hoffman in 1935, and contains layers of Sn and S atoms tightly bound together while the bonding between layers is of the weak van der Waals type [1]. Many investigations on the electrical, optical and photoconductivity properties of SnS single crystals have been carried out up to now [2–6]. It has been found that SnS crystals exhibit photoconductivity for wavelengths less than ~1.2 μm and the hole mobility is 90 $cm^2\ V^{-1}\ s^{-1}$ perpendicular to the c-axis. The absorption coefficient is $\sim 10^4\ cm^{-1}$ near the fundamental absorption edge, which allows absorption of light even for a small thickness.

In particular, within the last few years SnS films have been prepared using several methods and characterized for different applications [7–15]. Values of an optical band gap of 1.36 eV and a high absorption coefficient, $\sim 10^5\ cm^{-1}$, have been reported. This compound crystallizes in an orthorhombic double-layered structure with lattice parameters of $a = 0.385$, $b = 1.142$ and $c = 0.438$ nm. Compared to other semiconductor compounds, it is much less toxic, cost effective and is stable in slight acidic media. It can be synthesized by using simple procedures such as spray pyrolysis and chemical bath techniques.

Our recent investigations on thermally evaporated micron-thick (~0.5 μm) SnS films demonstrated that the films grown at a substrate temperature of above 275 °C exhibited single-phase nature with a nearly stoichiometric chemical composition between Sn and S. These films showed an electrical resistivity of 35.6 Ω cm with an optical band gap of 1.35 eV at room temperature. Any optoelectronic device requires an absorber layer with a high absorbance and a low resistivity. In general, the resistivity of the films strongly depends on preparation conditions and techniques. However, an effective way to obtain low-resistive films is by creating an excess of metal atoms through various heat treatments and/or incorporation of suitable dopants [16]. Therefore, we planned to achieve low-resistive SnS films in both ways, namely heat treatment and incorporation of metal dopants. In this paper, we report for the first time the effect of annealing on the physical properties such as composition, structural, optical and electrical behaviour of evaporated SnS films.

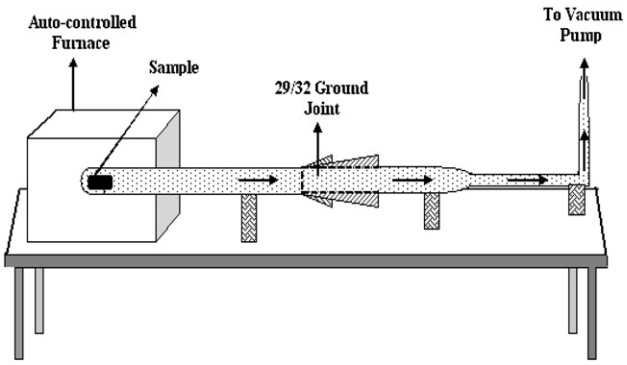

Figure 1. Schematic diagram of the annealing set-up.

2. Experimental procedures

The SnS films were deposited using a thermal evaporation technique on Corning 7059 glass substrates. SnS compound with 4N purity was evaporated from a molybdenum boat by applying a constant voltage and current of 32 V and 75 A, respectively. The depositions were carried out in a high vacuum system at a partial pressure of 10^{-6} Torr. The other deposition parameters such as substrate temperature, distance between source and substrates, rate of deposition and films' thicknesses were kept constant at 300 °C, 14 cm, 10 Å s^{-1} and ∼0.5 μm, respectively. The as-deposited SnS films were annealed at different temperatures of 100, 200, 300 and 400 °C for 1 h under a vacuum of 10^{-5} Torr in a home-built furnace. The schematic diagram of the furnace set-up is shown in figure 1.

The elemental composition of the annealed SnS films was examined using SEM attached with the EDAX system (model: FEI Sirion). The structural features have been checked using the XRD spectra collected from an x-ray diffractometer (model: Phillips X'Pert Pro). The surface topology and morphology of the annealed SnS films were examined using SEM (model: FEI Sirion) and AFM (model: Digital Instrument Nanoscope-E) in contact mode. In order to study the current transport mechanism in the films, current–voltage (*I–V*) characteristics have been investigated at room temperature. They were measured in the dark using the van der Pauw method in the dc voltage range, 0.0–1.0 V. The voltage was supplied and the corresponding output current was measured with a Keithley electrometer (model: 6517A). The temperature-dependent resistance studies were also carried out with the above-mentioned electrometer in the temperature range 20–250 °C using a two-probe technique. The temperature was controlled using a temperature controller with an accuracy of ±2 °C. The transmittance and reflectance spectra of the SnS films have been recorded as a function of wavelength by an FTIR spectrometer (model: Bruker IFS 66V/S) in the wavelength range 500–2500 nm with an incident light perpendicular to the cleavage plane of the film.

3. Results and discussions

The SnS films annealed at different temperatures were pinhole free, smooth and strongly adherent to the surface of the substrate. The change of colour of the films is negligible. However, the films annealed at 400 °C exhibited a discontinuity (in a few places) in the film due to re-evaporation of SnS itself. It is generally recommended that T_a of any material should be less than one-third of its melting point [17–20]. Since the melting point of SnS is ∼900 °C, therefore T_a should be ⩽300 °C. It might be the cause of the above observation.

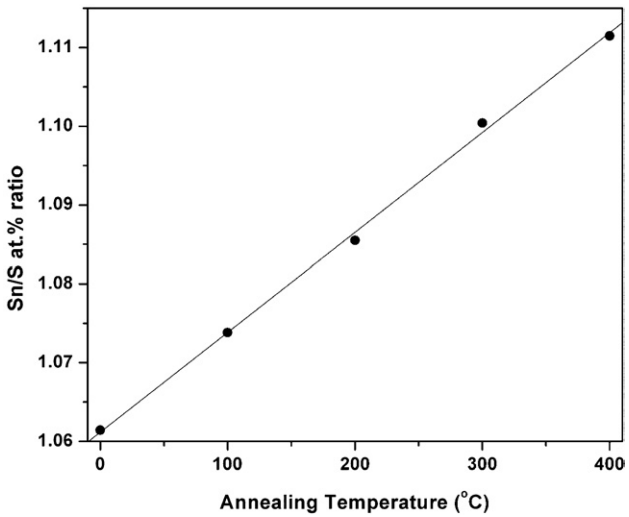

Figure 2. Variation of Sn/S ratio with respect to annealing temperature.

3.1. Composition analysis

The variation of Sn to S atomic ratio of the SnS films with respect to the annealing temperature is shown in figure 2. The Sn/S ratio (at%) increased from 1.06 to 1.11 with the increase of T_a, i.e. the sulfur content in the films decreased at higher annealing temperatures. The estimated sulfur content in the films decreased from 48.51 at% for as-deposited films to 47.36 at% for those annealed at 400 °C. Deficiency of sulfur might be attributed to re-evaporation of sulfur from SnS layers with T_a because of its high vapour pressure. The rate of change of Sn/S at% ratio is 1.27×10^{-4} °C^{-1}. Therefore, the annealed films are slightly sulfur deficient compared to as-deposited films (figure 2).

3.2. Structural analysis

3.2.1. Structural properties. The XRD spectrum of the as-deposited SnS films exhibited peaks related to different orientations at $2\theta = 26.12°$, 27.47°, 30.57°, 31.56°, 39.01°, 45.46°, 53.22° and 64.21°. These films showed an orthorhombic structure and the calculated lattice parameters are $a = 0.429$, $b = 1.123$ and $c = 0.399$ nm. The lattice parameters (a, b and c) were evaluated using the standard equation for an orthorhombic crystal structure, $1/d^2 = h^2/a^2 + k^2/b^2 + l^2/c^2$, where d is the space between lattice planes and (h, k, l) are the Miller indices. The change of lattice parameters a, b and c with T_a is marginal. The evaluated d-spacing and lattice parameters are very closely matching with the standard JCPDS data (no. 39-0354). The XRD spectra of SnS films annealed at different temperatures are shown in

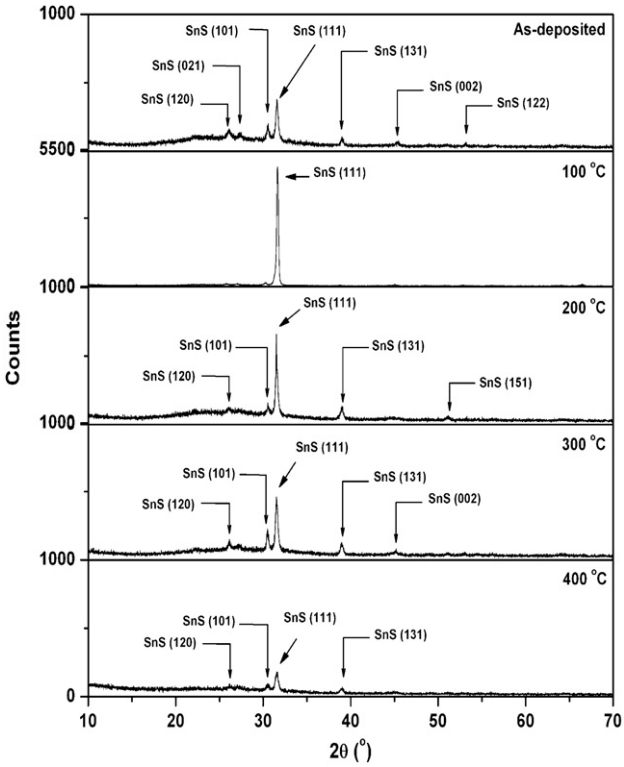

Figure 3. XRD spectra of the SnS films annealed at different temperatures.

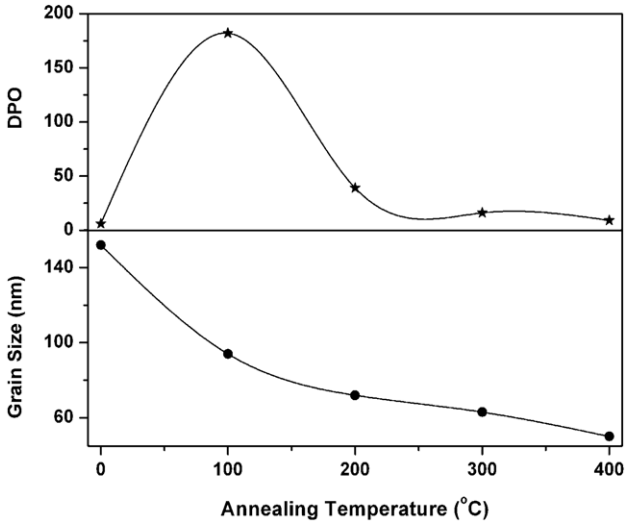

Figure 4. Variation of grain size and DPO of the SnS films as a function of annealing temperature.

figure 3, where the peaks identified using the above JCPDS data are labelled with the corresponding orientations. There is no change in the structure of the SnS films with T_a. Both the as-deposited and annealed films showed a peak diffracted at 31.56° corresponding to the (1 1 1) plane, as the preferred orientation, compared to other planes.

3.2.2. Grain size (L) and degree of preferred orientation (DPO). Figure 4 shows the variation of average grain size and degree of preferred orientation of the films with T_a

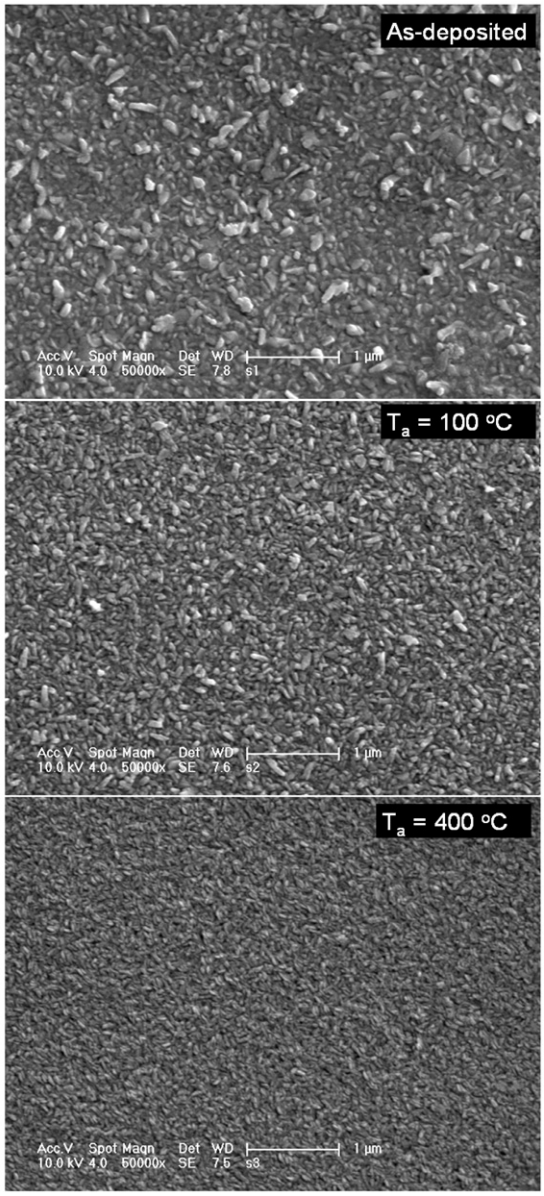

Figure 5. SEM pictures of the SnS films as deposited, $T_a = 100$ °C and $T_a = 400$ °C.

evaluated using standard equations [21, 22]. The grain size of the SnS films decreased from 152 nm to 50 nm with the increase of T_a. However, the DPO initially increased and reached a maximum value of 182 at the annealing temperature of 100 °C. Above this temperature, it decreased. The decrease of average grain size with T_a might be due to the fragmentation of clusters of crystallites. Such a decrease of grain size is clearly observed in the surface structure analysis given below. However, most of the fragmented crystallites are oriented in the (1 1 1) direction.

3.3. Surface structure

3.3.1. Surface topology. The SEM studies on SnS films demonstrate that the surface topology of the films is dependent on annealing temperature. Figure 5 shows the SEM

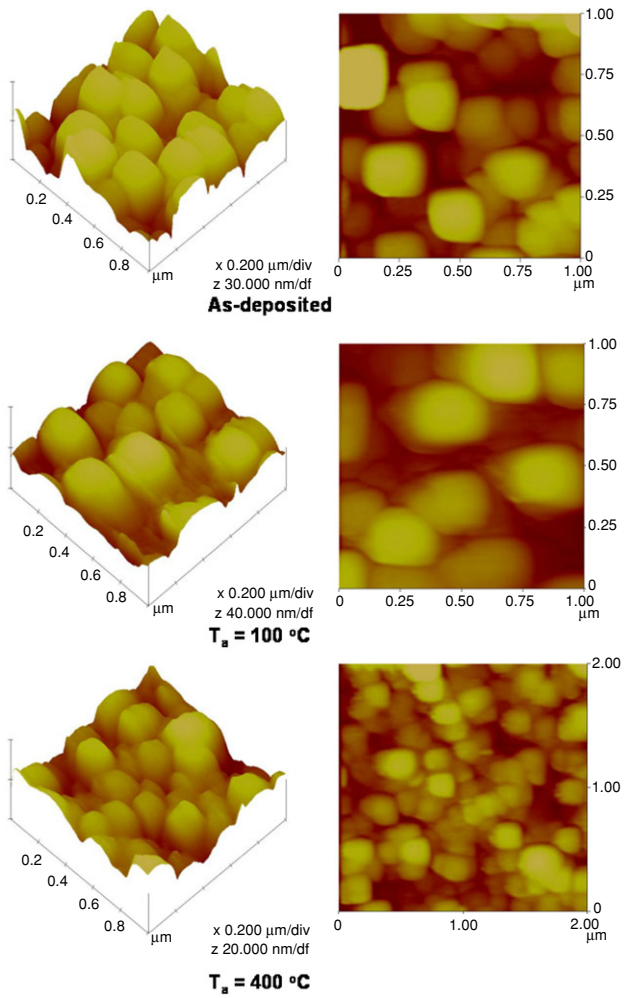

Figure 6. AFM pictures of the SnS films as deposited, $T_a = 100$ °C and $T_a = 400$ °C.
(This figure is in colour only in the electronic version)

micrographs of the as-deposited, annealed SnS films at 100 and 400 °C. A gradual change in the growth of crystallites from island nature to densely packed nature is seen with the increase of T_a. These crystallites are oriented randomly and the gaps between crystallites are reduced with increase of T_a and so the crystallites form a densely packed network. The density of crystallites is increased with the increase of T_a. The surface of the SnS films annealed at 400 °C looks smooth in nature.

3.3.2. Surface morphology. The AFM pictures, recoded in the area of 1 μm × 1 μm, are shown in figure 6. It shows the presence of square-shaped stubs on the top of a homogeneous granular surface. This indicates the surface roughness of the films. Initially, the stubs are nicely square in shape. This regular shape of the crystallites is suppressed with the increase of T_a. These pictures indicate clearly how the shape of the top of the grain surface changes with the increase of T_a. The plane view of 2D pictures reveals the formation of clusters of crystallites and change in grain size with the annealing temperature. The variation of the grain size and surface roughness of the SnS films extracted from AFM

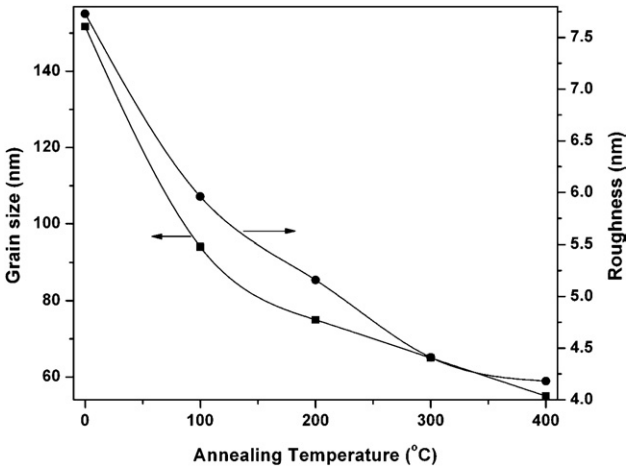

Figure 7. Variation of grain size and roughness of the SnS films with respect to annealing temperature.

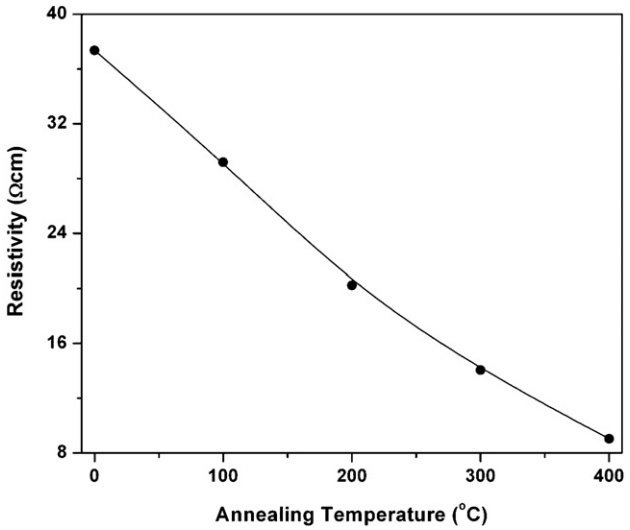

Figure 8. Variation of electrical resistivity of the SnS films with respect to annealing temperature.

pictures are shown in figure 7. With the increase of T_a the average rms value of roughness of the SnS films decreased from ∼7.73 nm for as-deposited films to a value of ∼4.18 nm for SnS films annealed at 400 °C. However, the evaluated grain size values match with the XRD data given earlier in figure 4. Clearly the fragmentation of grains increased with the increase of annealing temperature.

3.4. Electrical properties

3.4.1. Electrical resistivity. The variation of electrical resistivity of SnS films as a function of T_a is shown in figure 8. The resistivity of the as-deposited SnS films decreased from the initial value of ∼37.4 to 9 Ω cm with the increase of T_a. In general, the resistivity of thin films depends on film thickness, composition and/or grain size. Here, the film thickness is constant and the changes in grain size have only a small effect on the resistivity. The main variation in electrical resistivity of the SnS films arises from the change in composition. According to EDAX analysis, the sulfur content in the films

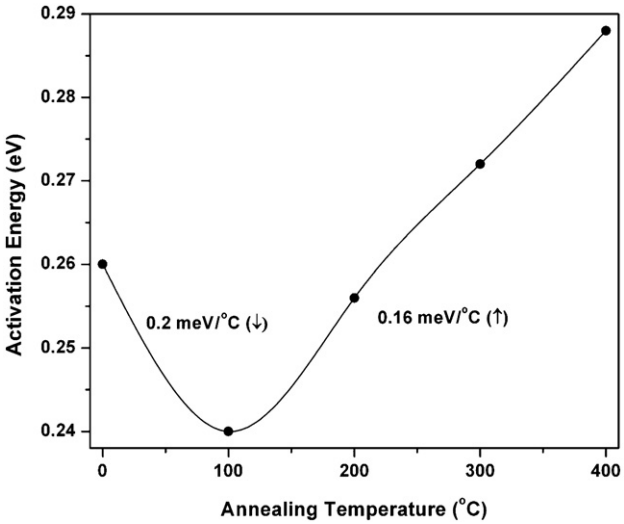

Figure 9. Variation of activation energy of SnS films with respect to annealing temperature.

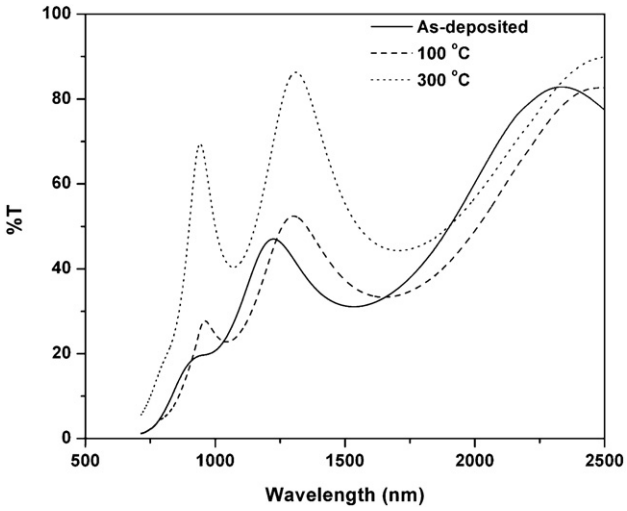

Figure 10. Transmittance versus wavelength of annealed SnS films.

decreased with the increase of T_a, resulting in tin richness of the films. The presence of excess tin might create excess of charge carriers in the films, leading to low resistivity. Consequently, the films annealed at 400 °C exhibited very low resistivity.

3.4.2. Activation energy. The temperature-dependent electrical resistivity of the annealed SnS films has been measured in the temperature range 20–250 °C. It decreases exponentially with the increase of temperature. The activation energy of the films was evaluated using semi-log plots of normalized conductivity (σ/σ_o) versus inverse absolute temperature ($1/T$). The plots are linear, indicating the extrinsic nature of the semiconductor. The extrinsic behaviour is due to the charge carriers liberated from the impurity levels. The variation of activation energy (ΔE) with the increase of annealing temperature is shown in figure 9. As-deposited SnS films exhibited an activation energy of 0.26 eV which matches with the data reported by Tanusevski *et al* [23] for the SnS films grown by electron beam evaporation. With the increase in T_a, the activation energy initially decreased and reached a minimum value of 0.24 eV at the annealing temperature of 100 °C. Above this annealing temperature, the activation energy increased and reached a maximum value of 0.29 eV at the annealing temperature, 400 °C. The activation energy of the SnS films is attributed to deep acceptor states due to Sn vacancies [24] that play a significant role in establishing the p-type conductivity of these compounds. In our earlier studies, we found activation energy of SnS films as 0.35 eV [25]. Noguchi *et al* [26] observed the activation energy, between 0.28 eV and 0.34 eV in thermally evaporated SnS films. However, Lopez *et al* [27] reported an activation energy of 0.54 eV for sprayed SnS films. Therefore, the activation energy of the SnS films depends on the film thickness, the deposition technique and film composition. The nature of the impurities responsible for the different values of activation energy requires further study.

3.5. Optical properties

The optical spectra of SnS films showed that the transmittance of the films increased with the increase of T_a. The films annealed at 400 °C showed a maximum transmittance of ~90% at a wavelength of 2500 nm as shown in figure 10. The appearance of interferences fringes is an indication of the thickness uniformity of the thin films. As-deposited films had a smaller slope of the transmittance curve, but with the increase of temperature its value increased and shifted to shorter wavelengths. It can be observed that an increase in the temperature improved the transmission, which can be due to either the decrease in thickness or stoichiometry of the SnS films.

3.5.1. Absorption coefficient and energy band gap. The absorption coefficient (α) of SnS films evaluated from transmittance versus wavelength data is $>3 \times 10^4\ \mathrm{cm}^{-1}$ above the fundamental absorption edge. α versus photon energy plots depicts that the optical transition (between the valence band and conduction band) in the films is direct because α varies rapidly as the photon energy increases [28]. The optical band gap (E_g) of the films was determined using $(\alpha h\nu)^2$ versus photon energy ($h\nu$) plots by extrapolating the plots onto $(\alpha h\nu)^2 = 0$. The variation of E_g with T_a is shown in figure 11. The optical band gap of the films initially decreased slightly from 1.37 eV for the as-deposited films to a value of 1.35 eV for the films annealed at 100 °C. Above this temperature, it increased and reached a value of 1.42 eV for the films annealed at 400 °C. Sharma *et al* [29] obtained optical band gaps of 1.4 eV and 1.38 eV for amorphous and crystalline SnS films grown by the thermal evaporation technique. Tanusevski [30] studied the optical behaviour of SnS films grown by a chemical bath deposition technique and annealed in argon environment for 1 h at different temperatures and reported that the direct band gap (1.38 eV) of the SnS films is independent of thermal treatment. The variation of activation energy and optical band gap of SnS films with T_a is more or less similar. This can be understood with the help of variation of DPO evaluated in the XRD studies. The DPO value is higher for SnS films

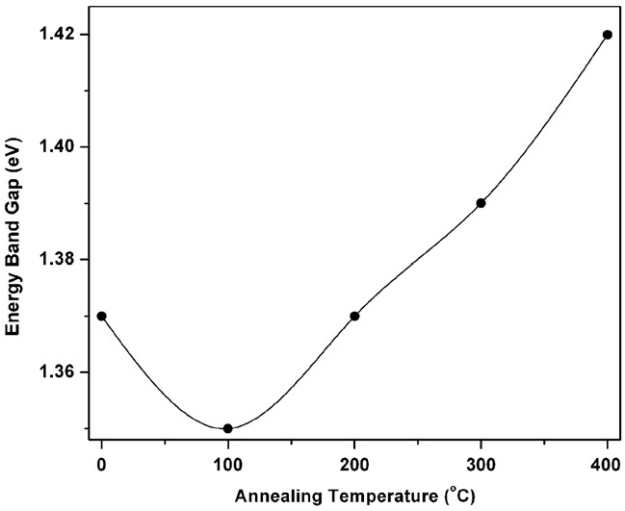

Figure 11. Variation of optical band gap of SnS films with respect to annealing temperature.

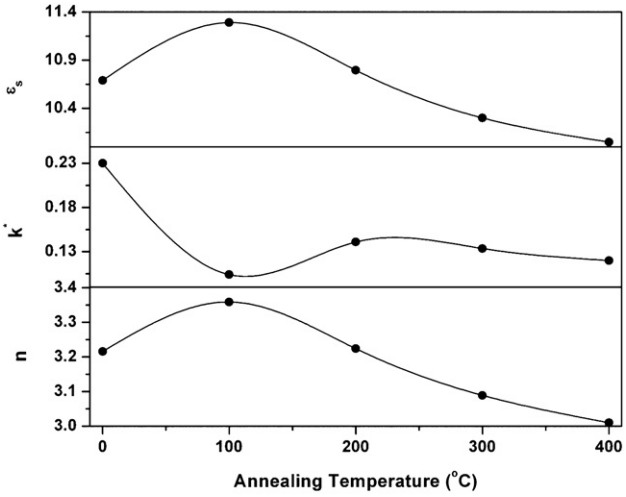

Figure 12. Variation of refractive index, extinction coefficient and static dielectric constant of the SnS films as a function of annealing temperature.

annealed at 100 °C than for the other films. This high DPO might be a reason for low values of activation energy and optical band gap of SnS films annealed at 100 °C. It is known, for example Ristov *et al* [24], that the optical band gap of the SnS films can be changed by varying the degree of crystallinity.

3.5.2. Refractive index (n), extinction coefficient (k) and static dielectric constant (ε_s).* The variation of optical parameters such as n, k^* and ε_s with the annealing temperature is shown in figure 12. The refractive index of SnS films increased from 3.22 with the increase of T_a and reached a maximum value of 3.36 at 100 °C. Above this temperature, it decreased and the films annealed at 400 °C showed a low value (3.01). The static dielectric constant also varied similarly with the increase of T_a. The SnS films annealed at 100 °C showed a high ε_s value (11.29). The extinction coefficient, however, showed different behaviour. The films annealed at 100 °C exhibited a low value (0.104) compared to the films annealed at other temperatures. These features of the films annealed at 100 °C might be due to high DPO.

4. Conclusions

The present work has attempted a study of the physical properties of SnS films annealed at different temperatures. With the increase of annealing temperature, the composition of the films changed due to the re-evaporation of sulfur. The films annealed at 400 °C showed an Sn/S atomic per cent ratio of ∼1.1. The structure of the SnS films remains unaffected and the change in lattice parameters is marginal. The grain size and roughness of the films decreased. As-deposited SnS films exhibit an electrical resistivity of 37.4 Ω cm, an optical band gap of 1.37 eV with an activation energy of 0.26 eV and a refractive index value of 3.22. However, the films annealed at 100 °C have a low activation energy (0.24 eV) and optical band gap (1.35 eV) with a high refractive index (3.36) and a low extinction coefficient (0.104) as compared with the films annealed at other temperatures. These films exhibited an electrical resistivity of 29 Ω cm.

Acknowledgments

The authors wish to thank K Anandhan, Glass blower, Department of Instrumentation, IISc, Bangalore for his efforts in the development of a simple and cost-effective annealing setup. We thank Professor Z Ivanova, Institute of Solid State Physics, Bulgaria, for technical discussion and suggestions. We also thank the referees for their useful suggestions.

References

[1] Elkorashy A M 1991 *Physica* B **168** 257
[2] Albers W, Haas C, Vink H J and Wasscher J D 1961 *J. Appl. Phys.* **32** 2220
[3] Albers W, Haas C and van der Maesen E 1960 *J. Phys. Chem. Solids* **15** 306
[4] Bilenkii B F, Mikolaichuk A G and Freik D M 1968 *Phys. Status Solidi* b **28** K5
[5] Lambros A P, Geraleas D and Economou N A 1974 *J. Phys. Chem. Solids* **35** 537
[6] Chamberlain J M and Merdan M 1977 *J. Phys. C: Solid State Phys.* **10** L571
[7] Pramanik P, Basu P K and Biswas S 1987 *Thin Solid Films* **150** 269
[8] Nair P K, Nair M T S, Zingaro R A and Meyers E A 1994 *Thin Solid Films* **239** 85
[9] Zainal Z, Hussein M Z and Ghazali A 1996 *Solar Energy Mater. Solar Cells* **40** 347
[10] Ray S C, Karanjai M K and Gupta D D 1999 *Thin Solid Films* **350** 72
[11] Ichimura M, Takeuchi K, Ono Y and Arai E 2000 *Thin Solid Films* **361** 98
[12] El-Nahass M M, Zeyada H M, Aziz M S and El-Ghamaz N A 2002 *Opt. Mater.* **20** 159
[13] Subramanian B, Sanjeeviraja C and Jayachandran M 2003 *Solar Energy Mater. Solar Cells* **79** 57
[14] Sato N, Ichimura M, Arai E and Yamazaki Y 2005 *Solar Energy Mater. Solar Cells* **85** 153
[15] Koteeswara Reddy N and Ramakrishna Reddy K T 2005 *Physica* B **368** 25
[16] Raghavan V 1999 *Materials Science and Engineering* 4th edn (New Delhi: Prentice-Hall) p 181

[17] Movchan B A and Demchishin A 1969 *Phys. Met. Metallogr.* **28** 83
[18] Thornton J A 1977 *Ann. Rev. Mater. Sci.* **7** 239
[19] Schoenmaker-Stolk M C, Verwijs J W and Scholten J J F 1987 *Appl. Catal.* **29** 91
[20] Monch W 1977 *Surf. Sci.* **63** 79
[21] Chopra K L 1969 *Thin Film Phenomena* (New York: McGraw-Hill) p 270
[22] De C K and Mishra N K 1997 *Indian J. Phys. A: Math. Gen.* **71** 530
[23] Tanuševski A and Poelman D 2003 *Solar Energy Mater. Solar Cells* **80** 297
[24] Ristov M, Sinadinovski Gj, Grozdanov I and Mitreski M 1989 *Thin Solid Films* **173** 53
[25] Koteeswara Reddy N and Ramakrishna Reddy K T 1998 *Thin Solid Films* **325** 4
[26] Noguchi H, Setiyadi A, Tanamura H, Nagatomo T and Omoto O 1994 *Solar Energy Mater. Solar Cells* **35** 325
[27] Lopez S and Ortiz A 1994 *Semicond. Sci. Technol.* **9** 2130
[28] Orton J 2004 *The Story of Semiconductors* (New York: Oxford University Press) p 66
[29] Shama A A and Zeyada H M 2003 *Opt. Mater.* **24** 555
[30] Tanusevski A 2003 *Semicond. Sci. Technol.* **18** 501